2010

Polymer length distributions for catalytic polymerization within mesoporous materials: Non-Markovian behavior associated with partial extrusion

Da-Jiang Liu
Ames Laboratory, dajiang@fi.ameslab.gov

Hung-Ting Chen
Iowa State University

Victor S.-Y. Lin
Iowa State University

James W. Evans
Iowa State University, evans@ameslab.gov

Polymer length distributions for catalytic polymerization within mesoporous materials: Non-Markovian behavior associated with partial extrusion

Abstract
We analyze a model for polymerization at catalytic sites distributed within parallel linear pores of a mesoporous material. Polymerization occurs primarily by reaction of monomers diffusing into the pores with the ends of polymers near the pore openings. Monomers and polymers undergo single-file diffusion within the pores. Model behavior, including the polymer length distribution, is determined by kinetic Monte Carlo simulation of a suitable atomistic-level lattice model. While the polymers remain within the pore, their length distribution during growth can be described qualitatively by a Markovian rate equation treatment. However, once they become partially extruded, the distribution is shown to exhibit non-Markovian scaling behavior. This feature is attributed to the long-tail in the "return-time distribution" for the protruding end of the partially extruded polymer to return to the pore, such return being necessary for further reaction and growth. The detailed form of the scaled length distribution is elucidated by application of continuous-time random walk theory.

Keywords
Catalytic polymerization, Continuous-time random walk theories, Kinetic Monte Carlo simulation, lattice models, length distributions, Markovian, polymer length, pore openings, rate equations, scaling behavior, single file diffusion, mesoporous materials, monomers, polymerization, silicon dioxide, algorithms

Disciplines
Mathematics | Physical Chemistry | Physics

Comments
The following article appeared in *Journal of Chemical Physics* 132, 15 (2010): 154102 and may be found at doi: 10.1063/1.3361663.

Polymer length distributions for catalytic polymerization within mesoporous materials: Non-Markovian behavior associated with partial extrusion

Da-Jiang Liu, Hung-Ting Chen, Victor S.-Y. Lin, and J. W. Evans

Citation: The Journal of Chemical Physics **132**, 154102 (2010); doi: 10.1063/1.3361663
View online: http://dx.doi.org/10.1063/1.3361663
View Table of Contents: http://scitation.aip.org/content/aip/journal/jcp/132/15?ver=pdfcov
Published by the AIP Publishing

Polymer length distributions for catalytic polymerization within mesoporous materials: Non-Markovian behavior associated with partial extrusion

Da-Jiang Liu,[1] Hung-Ting Chen,[1,2] Victor S.-Y. Lin,[1,2] and J. W. Evans[1,3,a)]
[1]*Ames Laboratory (USDOE), Iowa State University, Ames, Iowa 50011, USA*
[2]*Department of Chemistry, Iowa State University, Ames, Iowa 50011, USA*
[3]*Departments of Physics and Astronomy and Mathematics, Iowa State University, Ames, Iowa 50011, USA*

(Received 12 November 2009; accepted 19 February 2010; published online 15 April 2010)

We analyze a model for polymerization at catalytic sites distributed within parallel linear pores of a mesoporous material. Polymerization occurs primarily by reaction of monomers diffusing into the pores with the ends of polymers near the pore openings. Monomers and polymers undergo single-file diffusion within the pores. Model behavior, including the polymer length distribution, is determined by kinetic Monte Carlo simulation of a suitable atomistic-level lattice model. While the polymers remain within the pore, their length distribution during growth can be described qualitatively by a Markovian rate equation treatment. However, once they become partially extruded, the distribution is shown to exhibit non-Markovian scaling behavior. This feature is attributed to the long-tail in the "return-time distribution" for the protruding end of the partially extruded polymer to return to the pore, such return being necessary for further reaction and growth. The detailed form of the scaled length distribution is elucidated by application of continuous-time random walk theory. © *2010 American Institute of Physics*. [doi:10.1063/1.3361663]

I. INTRODUCTION

For more than a decade, there has been sustained interest in the utilization of mesoporous materials to facilitate production and processing of polymeric materials with desired higher-order structures,[1] e.g., linear "molecular wires" versus more complex cross-linked networks. The current investigation is motivated primarily by experiments demonstrating the successful fabrication of molecular wires of poly(phenylene butadyiene) or PPB encapsulated within a Cu^{2+}-functionalized MCM-41 silica, a mesoporous silica nanosphere material.[2] The success of this catalytic nanoreactor derived in part from the application of a cocondensation procedure[3] which resulted in the copper catalyst sites being distributed "homogeneously" within the pores. In contrast, cross-linked polymer configurations resulted from traditional direct grafting followed by impregnation methods which produced a large portion of catalytic sites distributed on the exterior surface of the nanospheres. In addition, it is significant for the current study to note that under typical reaction conditions for production of PPB in this system, polymers tend to ultimately clog the pores rather than being completely extruded.[2]

Since the mesopores in the MCM-41 silica system have a small diameter of ~2.5 nm in the polymerization experiments,[2] one expects that diffusive transport of monomers and PPB polymers within the pores may exhibit some anomalous features associated with one-dimensional (1D) "single-file" systems[4] and also be affected by strong interaction with the pore.[5,6] Thus, our previous modeling of this system[7] incorporated this single-file feature, and also naturally included a decrease in polymer diffusivity with increasing length.[8,9] In addition, our modeling also specified diffusion-limited reaction kinetics wherein polymerization occurred instantaneously but only when the ends of polymers and/or monomers met at a catalytic site.

We now briefly describe the basic model behavior for moderate rates of monomer input to the pore and for strongly decreasing polymer diffusivity with increasing length. A more detailed description is presented in Sec. II. After a transient period, a configuration is reached dominated by one large polymer near each end of the pore. Thereafter, growth of this long polymer generally occurs in two stages, see Fig. 1. In the first stage, polymer growth is achieved primarily within the pore. The second stage is realized after the polymer has grown longer than the typical separation between catalytic sites. Then, the end of the polymer often leaves the pore (partial extrusion), further reaction and growth occurring only when this end returns to the pore. A standard Markovian rate equation analysis (see Sec. III) demonstrates distinct scaling for the growth of the mean polymer length in each of the above two stages. An extended Markovian rate equation analysis for the distribution of lengths seems partly effective recovering Poisson-like behavior in the first stage, but completely fails to describe distinct scaling behavior in the second stage.

Our focus will be on elucidating the latter failure or discrepancy. We describe this as non-Markovian behavior of the polymer length distribution occurring in the presence of partial extrusion. We use the term non-Markovian to mean that the evolution of this length distribution is not described by standard Markovian rate equations. This is perhaps surprising since our complete model for polymerization, involving stochastic diffusion of multiple monomers and polymers together with polymerization reaction at catalytic sites, is cer-

a)Electronic mail: evans@ameslab.gov.

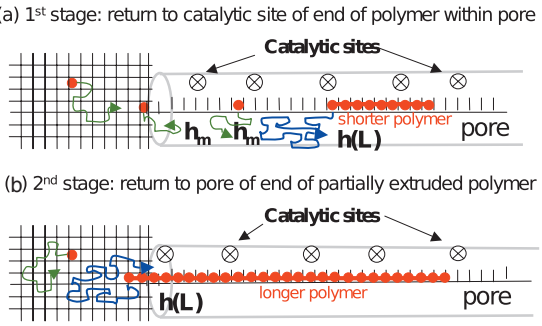

FIG. 1. Schematic of two regimes of polymer growth: (a) polymerization within the pore (quasi-Markovian kinetics) and (b) polymerization with partial extrusion (non-Markovian kinetics). Diffusion of monomers and polymers within the pore, and of partially extruded polymers, is one-dimensional.

tainly Markovian. However, the non-Markovian behavior applies to a reduced variable, the polymer length. We shall see that the key feature inducing non-Markovian behavior is that the distribution of waiting times between polymer growth events has a long time tail, and specifically that the mean waiting time diverges for long polymers. It is instructive to note more generally that when developing a closed formulation for the dynamics of a reduced set of variables, one generally expects to generate non-Markovian (or irreversible) behavior even if the full model is Markovian (or time-reversal invariant). This general feature is familiar from Mori–Zwanzig projection operator formalisms[10,11] and the associated Mori–Kubo generalized Langevin equations,[10,12] or from the Brussels' school formulation of subdynamics.[13]

In Sec. II, we describe our general model for polymerization, our discrete space implementation of the model and associated kinetic Monte Carlo (KMC) simulation algorithm, as well as basic model behavior. In Sec. III, we present simulation results together with a Markovian rate equation analysis for behavior in our general model. The successes and shortcomings of this analysis are also described. Next, in Sec. IV, we briefly describe an analytic formulation for our model in the regime of high (maximal) catalyst loading where partial extrusion predominates and the Markovian rate equation treatment completely fails. Then, in Sec. V, we present simulation results together with a complete and exact non-Markovian analysis of a tailored model for maximal catalysts loading which neglects complete polymer extrusion. The latter analysis successfully elucidates the scaling behavior of the polymer length distribution. Conclusions are provided in Sec. VI.

II. GENERAL POLYMERIZATION MODEL, KMC ALGORITHM, AND BASIC BEHAVIOR

A. Key model ingredients

Our model[7] includes a source of monomers exterior to the pores. These monomers diffuse into the pores and undergo polymerization reaction at catalytic sites within the pores. Polymers thus formed can undergo further polymerization reaction at catalytic sites with monomers or other polymers, and potentially be extruded from the pores. A more comprehensive description of the key model ingredients follows prescribing both the diffusive transport and reaction kinetics:

(i) Diffusive transport. We treat monomer and polymer diffusion within the pores as purely 1D with a "no-passing" (single-file) constraint. Furthermore, the polymer diffusion coefficient is assumed to decrease algebraically with polymer length.[8,9] Diffusion-mediated polymer extrusion is possible, although improbable for long slowly diffusing polymers. In our modeling, once completely extruded, the polymer cannot return into the pore due to orientational misalignment. We also assume that partly extruded polymers undergo unbiased diffusion, just as when completely within the pore. Any entropic driving force for extrusion (due to access to a larger number of polymer configurations in the fluid) would introduce a slight outward diffusion bias. However, PPB polymers are quite stiff, so this driving force should be very weak.

(ii) Polymerization kinetics. We stipulate that the polymerization reaction can occur only when the ends of polymers and/or monomers meet at a catalytic site within the pore. When this configuration is achieved, reaction is assumed to occur instantaneously, i.e., reaction is diffusion limited. The catalytic sites are taken to be distributed periodically along the pore given the characteristics of the cocondensation procedure described in Sec. I. Monomer input to a pore is possible provided that the end of the pore is not blocked by polymers (or monomers). This input is fed by a constant concentration of monomers within the surrounding fluid.

B. Discrete implementation and KMC algorithm

For convenience, we implement the above processes within a spatially discrete one-dimensional lattice model. This approach has already been successfully applied for reaction-diffusion processes in mesoporous systems with single-file diffusion.[7,14] In our formulation, monomers and polymers reside on individual sites or adjacent strings of sites on this lattice which runs through the pore. The lattice constant is taken as the monomer dimension, and all lengths below are quoted in lattice constants (so polymer lengths are measured in monomers). Diffusive transport is described by monomers as well as polymers hopping left or right to neighboring sites within the pore. The discreteness should not affect the basic model behavior, particularly for the long times and significant diffusion lengths (relative to the monomer length) which are of primary interest in this work. We will denote the length of the pore by L_p (=200 in our simulations). Catalytic sites are periodically distributed along the interior of the pore with a separation denoted by L_c.

Specific details of the diffusion and reaction kinetics are as follows. (i) Monomers are fed into the pore at rate x_{in} provided that the end site within the pore is not blocked (by a monomer or part of a polymer). (ii) The rate for monomers

hopping left or right within the pore is denoted by h_m. Below we set $h_m=1$ which identifies the characteristic time for monomer hopping as the unit of time.[15] (iii) We select the rate for polymers hopping left or right, h(L), to decrease with their length, L, according to the form $h(L)=h_m/L^{\alpha}$. The polymer diffusion exponent, α, describes the rate of decay.[9] (iv) Polymerization reaction occurs instantaneously when a pair of monomers, or when a monomer and the end of a polymer, or when the ends of a pair of polymers are on neighboring sites at the location of a catalytic site. (v) Partially extruded polymers also hop at rate h(L), with the constraint that they cannot return to the pore once completely extruded. These extruded polymers are regarded as diffusing away from the pore, and thus do not block entry of monomers to the pore.

The complex interplay between reaction and diffusion processes in the above nonequilibrium multispecies lattice-gas model is readily and efficiently analyzed via KMC simulation.[16–20] The key feature of these KMC simulations is that processes are implemented with probabilities proportional to their rates.

C. Basic model behavior

We now briefly review the basic behavior of the model as determined from our previous simulation study.[7] These observations will motivate our examination of specific fundamental issues in this paper. For moderate monomer input rates (around $x_{in}=0.01-0.1$ monomers per pore per unit time), and provided that the polymer diffusion coefficient decreases significantly with length ($\alpha \geq 1$), polymers tend to form near the pore openings. After a transient period, a configuration is reached dominated by one large polymer near each end of the pore. Thereafter, growth of this long polymer generally occurs in two stages. See again Fig. 1 for a schematic. In the first stage, polymer growth is achieved primarily within the pore. When the end of the polymer closest to the pore opening reaches a catalytic site, reaction typically occurs with a monomer which has diffused into the pore. The resulting growth shifts the end of the polymer away from the catalytic site. This end of the polymer then undergoes a random walk, subsequent reaction and growth likely occurring when it returns to the same catalytic site or reaches a neighboring catalytic site (typically the former). The second stage is achieved after the polymer has grown so that its length exceeds the typical separation between catalytic sites. Then, it becomes more likely that the end of the polymer will leave the pore, i.e., the polymer will become partly extruded. Now, further reaction and growth occurs only when the end of the polymer returns to the pore, or more specifically to the catalytic site closest to the end of the pore. There is a small chance for complete extrusion, in which case growth of another polymer is initiated.

III. KMC SIMULATION RESULTS AND ANALYSIS

Simulation results are presented here for the general polymerization model discussed in Sec. II. We consider a mesoporous system consisting of many parallel pores and regard the polymerization process as occurring independently

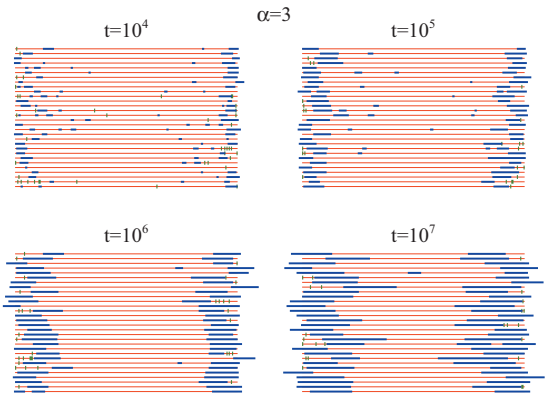

FIG. 2. Snapshots of polymer and monomer distributions within mesopores after various reaction times (shown) for $\alpha=3$ and $x_{in}=0.1$. Blue (narrower and longer) segments indicate polymers and green (wider and short) segments indicate monomers. The pore is indicated by a thin red line. Partial extrusion of many polymers is evident for longer times.

in the different pores. Below, N_L will denote the number of polymers of length L (measured in monomers) per pore in the system. Then, $N_p=\Sigma_{L>1}N_L$ denotes the total number of polymers per pore. Also, let L_{av} denote a suitably defined mean polymer length, as discussed further below. Then, it is convenient to write the polymer length distribution in the form[7,21]

$$N_L = (N_p/L_{av})f(L/L_{av}), \quad \text{with} \quad \int_{0<x<\infty} dx\ f(x) = 1. \quad (1)$$

Here, the scaling function f(x) describes the shape of the polymer length distribution. For L_{av}, one could choose the definition

$$L_{av} = \sum_{L>1} LN_L / \sum_{L>1} N_L = \sum_{L>1} LN_L/N_p \quad \text{implying} \quad \int_{0<x<\infty} dx x f(x) = 1. \quad (2a)$$

Instead, one could choose the (equally legitimate) alternative definition

$$L_{av} = \sum_{L>1} L^2 N_L / \sum_{L>1} LN_L \quad \text{implying} \quad \int_{0<x<\infty} dx f(x) = \int_{0<x<\infty} dx x f(x). \quad (2b)$$

The second choice Eq. (2b) corresponds to weighting by size or length, which is common in percolation-theoretic analyses of size distributions.[21] Results for the shape function f(x) depend only weakly on the choice, and we use the latter in this work. Any explicit dependence of f(x) on time, t (not shown), corresponds to a lack of scaling. We note that L_{av} generally increases with t producing an implicit dependence of N_L on t.

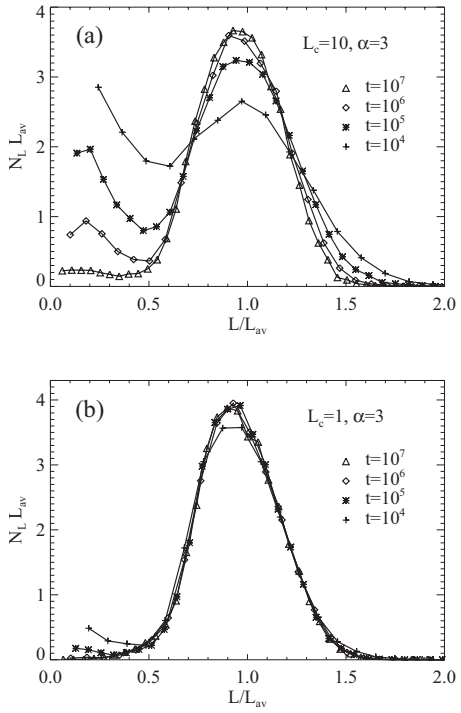

FIG. 3. Evolution of the scaled polymer length distribution for the general model for catalytic polymerization for $\alpha=3$ and $x_{in}=0.1$. Simulation results for (a) lower catalyst loading $L_c=10$ (polymerization primarily within the pore for shorter times); (b) maximal catalyst loading $L_c=1$ (polymerization with partial extrusion). The area under the curves corresponds to the typical number of polymers per pore, $N_p \approx 2-3$. Times are shown in the plots.

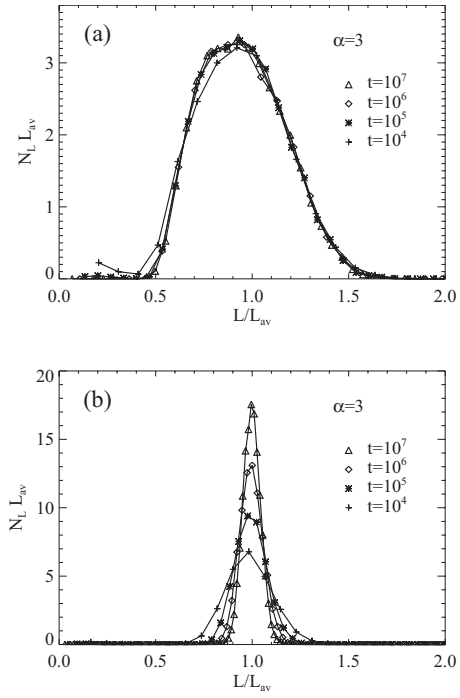

FIG. 4. Evolution of the scaled polymer length distribution for modifications of the general model for catalytic polymerization for $\alpha=3$ and $x_{in}=0.1$. Simulation results for imposition of (a) a "reflecting boundary condition" to block complete extrusion; (b) a severe constraint excluding even partial extrusion (so that the polymer remains completely within the pore). The area under the curves corresponds to $N_p \approx 2-3$. Times are shown in the plots.

A. KMC simulation results

In Fig. 2, we show the evolution with reaction time of the polymer and monomer distributions within an ensemble of pores for polymer diffusion exponent $\alpha=3$ with catalytic site separation $L_c=10$ and input rate $x_{in}=0.1$. Each frame in the figure is a composite plot of individual simulation trials for 30 pores. These are combined into a single ensemble representative of an array of pores within a MCM-41 material. One can see clearly the tendency of longer polymers to form and grow near the end of pores. Thus, the number of polymers per pore, N_p, is quite high for early times, but quickly decreases to $N_p \approx 2-3$ for moderate times, and approaches $N_p=2$ for very long times. We now describe in more detail the behavior of this general model for the two regimes corresponding to the two distinct stages mentioned in Sec. I:

(i) KMC simulation with lower catalyst loading corresponding to catalytic site separation $L_c=10$ reveals that at least for shorter times polymerization occurs primarily within the pore, the first stage described in Sec. II C. Previous simulation studies indicated rather well-defined temporal scaling of the mean polymer length of the form $L_{av} \sim t^{1/(\alpha+1)}$ at least for $\alpha \geq 2$.[7] Analysis of the polymer length distribution, N_L, reveals a lack of perfect scaling at least for shorter times, specifically f(x) evolves becoming sharper with increasing times. Results have been shown previously for $\alpha=2$ (Ref. 7) and are shown in Fig. 3(a) for $\alpha=3$. For longer times, results suggest that improved scaling is achieved, behavior characteristic of the second stage described below.

(ii) KMC simulation with high catalyst loading reveals that polymerization quickly leads to partial extrusion of the polymer, the second stage described in Sec. I. To most effectively probe this regime, we performed simulations in the extreme case of maximal loading with $L_c=1$ (i.e., all sites within the pore are catalytic). Simulations indicate well-defined scaling of the mean polymer length of the form $L_{av} \sim t^{1/(\alpha+2)}$ at least for $\alpha \geq 2$ (Ref. 7) which is distinct from that described for the first stage above. Analysis of the polymer length distribution, N_L, reveals near-perfect scaling, i.e., time invariant f(x). Results are shown in Fig. 3(b) for $\alpha=3$.

The lack of scaling in case (i) is expected from simple Markovian modeling described below. To provide more insight into the scaling behavior in case (ii), it is instructive to explore the influence on behavior of various model refinements. We retain maximal catalyst loading $L_c=1$. However, we first refine the model to forbid complete extrusion of the polymer by simply implementing a "reflecting" boundary condition on the associated random walk. Results shown in Fig. 4(a) for $\alpha=3$ reveal little change from behavior in the complete model, including retention of near-perfect scaling. In the second more extreme refinement, we forbid even partial extrusion, so the polymer remains completely within the pore as it grows. Results shown in Fig. 4(b) for $\alpha=3$ reveal a complete lack of scaling and instead a sustained sharpening of the distribution.

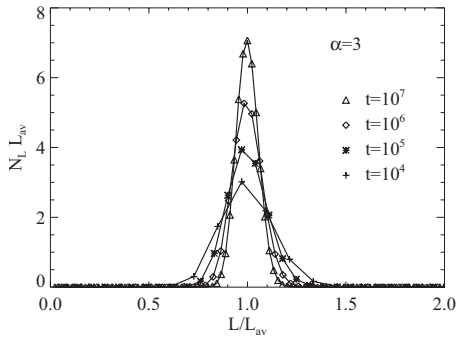

FIG. 5. Solution of the Markovian rate Eq. (4) with $P_{rx}=1$ for the evolution of the scaled polymer length distribution choosing $L_c=10$ and $\alpha=3$ and $x_{in}=0.1$. The area under the curves corresponds to $N_p=1$ in this analysis. Times are shown in the plot.

B. Markovian rate equation analysis

We start by elucidating behavior in the first stage of polymerization occurring primarily within the pore. After being shifted away from a catalytic site due to growth, the typical number of hops for the end of the polymer chain to return to a catalytic site is $\langle n_h \rangle \approx L_c$,[22–24] the separation between catalytic sites. We denote the probability for reaction and growth upon return as P_{rx}.[25] Then, the typical rate at which the end of a polymer of length L reacts to a catalytic site is given by $R(L) \approx P_{rx} h(L)/\langle n_h \rangle$, where again h(L) is the polymer hop rate for length L. Consequently, it follows that

$$d/dt \ L_{av} \approx R(L_{av}) \approx P_{rx} h(L_{av})/\langle n_h \rangle \sim (L_{av})^{-\alpha}. \quad (3)$$

This result is consistent with the observed scaling $L_{av} \sim t^{1/(\alpha+1)}$. Extending this Markovian-type rate equation analysis to consider the evolution of the polymer length distribution, one naturally writes

$$d/dt \ N_L \approx R(L-1)N_{L-1} - R(L)N_L. \quad (4)$$

Behavior of the solutions of these equations for $L_c=10$ and $x_{in}=0.1$ shown in Fig. 5 matches Fig. 4(b) and is qualitatively similar to the short-time behavior in Fig. 3(a). Deviations from quantitative predictive capability for the latter will be discussed in Sec. VI. In the special case n=0 where the polymer diffusivity independent of length, N_L from Eq. (4) evolves to a Poisson distribution for which the standard deviation scales like $(L_{av})^{1/2}$. This implies a sharpening of the function f(x) as seen in Fig. 5 or Fig. 4(a).

Next, we consider the second stage of polymerization where the polymer is partly extruded from the pore. Note that when a polymer of length L becomes partly extruded from the pore, a standard analysis of random walks in the presence of traps shows that there is a probability $P_{ex}=1/L$ for complete extrusion.[26] Thus, for long polymers, there is a high probability $P_{ret}=1-P_{ex}$ for return of the end of the polymer to a catalytic site within the pore leading to further reaction and growth (typically by more than one monomer). In this case, the average number of hops until returning will scale like $\langle n_h \rangle \sim L$ (cf. the number of hops for a walker returning to a single trap on a 1D lattice of L sites).[22,23] One thus obtains

$$d/dt \ L_{av} \approx P_{ret} \ h(L_{av})/\langle n_h \rangle|_{L=Lav} \sim (L_{av})^{-\alpha-1}, \quad (5)$$

which is consistent with the observed scaling $L_{av} \sim t^{1/(\alpha+2)}$. An alternative and more rigorous derivation of this behavior is provided in Sec. V. Note that there is also a loss term for $d/dt \ L_{av}$ due to complete extrusion polymer, and this term is of the same order as the above gain term.[27] Extending the Markovian-type rate equation analysis to consider the evolution of the polymer length distribution N_L (Ref. 28) fails to produce the scaling behavior observed in simulations. We shall describe in more detail the origin of this failure in the following sections.

IV. POLYMERIZATION WITH MAXIMAL CATALYST LOADING: GENERAL ANALYTIC FORMULATION

Our primary goal in this paper is to elucidate the breakdown of Markovian behavior and the scaling of N_L occurring in the second stage of polymerization involving partial extrusion. Since the formation of one long polymer occurs near each end of the pore in the general model, it suffices to analyze polymerization near the end of a semi-infinite pore (regarded as extending to the right). To enhance partial extrusion which underlies the above-mentioned breakdown, it is convenient to consider the case of maximal catalyst loading $L_c=1$ where all sites inside the pore are catalytic. Also, for simplicity, we consider only the regime of instantaneous reaction, $P_{rx}=1$,[7] when the end of the polymer is within the pore and thus at a catalytic site. In this model for a semi-infinite pore, we regard the number of polymers per pore as satisfying $N_p=1$.

To visualize the special behavior for maximal catalyst loading, imagine that the left end of a polymer of length L has just returned inside the left end of the semi-infinite pore and thus to a catalytic site (described succinctly below as returning to the pore). Then, it grows immediately by one monomer, and with probability $p_1=1/2$ then hops left out of the pore. In this case, the change in length is $\delta L=1$. With probability $p_m=(1/2)^m$, it hops right m−1 further times into the pore, each time immediately growing by another monomer, before hopping left out of the pore on the mth hop for an overall increase in length of $\delta L=m$. Thus, since $\Sigma_{m\geq 1} p_m=1$, the average increase in length during a "growth cycle" upon returning to the pore is $\langle \delta L \rangle = \Sigma_{m\geq 1} m \ p_m=2$.

After the (left end of) a polymer of length L departs (left end of) the pore, there are two possibilities. First, it can return to the pore with probability $P_{ret}(L)$ leading to another growth cycle. Second, it can be completely extruded with probability $P_{ex}(L)$, leading to formation of a new polymer of length L=2 at the end of the pore. One has that[22] $P_{ret}(L) + P_{ex}(L)=1$, where $P_{ex}(L)=1/L$, as noted in Sec. III B. Thus, for large L, growth by on average $\langle \delta L \rangle = 2$ with probability $P_{ret}(L) \approx 1$ dominates "antigrowth" by $\langle \delta L \rangle = -(L-2)$ with probability $P_{ex}(L)=1/L$.

For this model, one can track behavior in terms of growth cycles (the cumulative number of the returns of the polymer to the pore plus the cumulative number of complete extrusions), or in terms of the cumulative number of hops of the polymers, or in terms of continuous time (as used to

describe KMC simulation and rate equation results). We emphasize that these are just different ways to picture or analyze the same model. Below, we focus on the latter two.

A. Discrete-time picture (time measured in hops)

For this system, it is natural to consider measuring "time" in terms of the cumulative number of hops "n" taken by the partially extruded polymers. In this discrete-time formulation, one determines the polymer length distribution, $N_L(n)$, after various numbers of hops n. Interestingly, $N_L(n)$ is independent of the size dependence of polymer diffusivity (and thus of α). This contrasts the strong dependence on α of the polymer length distribution, $N_L(t)$ at fixed time (cf. Sec. V). This difference reflects the spread of times, t, associated with each fixed n (and we should also note the nonlinear relationship between n and t).

Within this discrete-time formulation, we introduce the return-time distribution, $F_{ret}^L(n)$, for return of a polymer of length L to the pore n hops after departing the pore. We choose the normalization $\Sigma_{n>0}F_{ret}^L(n)=P_{ret}(L)$, so then the mean return time (measured in hops) is given by $\langle n\rangle_{ret}=\Sigma_{n>0}n\ F_{ret}^L(n)/P_{ret}(L)$. For large L, where one can plausibly neglect complete extrusion, $F_{ret}^L(n)\approx F_n$ roughly corresponds to the return time distribution for a 1D random walk to return to the origin in exactly n hops. Behavior of this quantity can be determined[29–32] from the well-known form of its generating function, $F(z)=\Sigma_{n>0}z^nF_n=1-(1-z^2)^{1/2}$,[23] yielding

$$F_n \sim n^{-3/2}/(2\pi)^{1/2}, \quad \text{as even} \quad n\to\infty, \tag{6}$$

and trivially $F_n=0$ for odd n. One finds that $\Sigma_{n>0}F_n=1$, so that the walk "recurrent,"[23] i.e., it is certain to return to the origin (consistent with the neglect of complete extrusion). Despite this feature, the mean return time is infinite, i.e., $\langle n\rangle_{ret}=\Sigma_{n>0}n\ F_n=\infty$ due to the long-time tail in the distribution.[33] Due to finite polymer length L, $F_{ret}^L(n)$ deviates from Eq. (6). The typical number of hops until extrusion should scale like $\langle n\rangle_{ex}\sim L^2$. Thus, the long-time tail in $F_{ret}^L(n)$ should be[23] truncated for n above $\langle n\rangle_{ex}$. We must also introduce the distinct extrusion-time distribution, $F_{ex}^L(n)$, for extrusion on the nth hop normalized so that $\Sigma_{n>0}F_{ex}^L(n)=P_{ex}(L)$. This distribution should be peaked around $n=\langle n\rangle_{ex}$.

Combining the information in the introduction to Sec. IV regarding growth cycles with these waiting time distributions allows determination of $N_L(n)$. See the Appendix.

B. Continuous-time picture

For direct comparison with and interpretation of behavior in KMC simulations or in experiments, one should determine the polymer length distribution, $N_L(t)$, at various times "t." For this continuous-time stochastic walk formulation (denoted CTRW after replacing the term "stochastic" with "random"),[23,29] we introduce a return-time distribution, $F_{ret}^L(t)$, which describes the distribution of times between departure from the pore and return for a polymer of length L. We choose the normalization $\int dt\ F_{ret}^L(t)=P_{ret}(L)$, so that then $\langle t\rangle_{ret}=\int dt\ t\ F_{ret}^L(t)/P_{ret}(L)$ denotes the mean return time. Likewise, we must introduce a separate extrusion-time distribution, $F_{ex}^L(t)$, normalized so that $\int dt\ F_{ex}^L(t)=P_{ex}(L)$.

One can convert the discrete-time (n) formulation of Sec. IV A into the CTRW by introducing the waiting-time distribution for individual hops. For a polymer of length L with hop rate h(L), this distribution has an exponential form $F_{hop}^L(t)=h(L)\exp[-h(L)t]$. Then, precise conversion is possible exploiting general procedures for conversion from a discrete- to continuous-time RW.[23,29] However, given the typically large number of hops between returns at least for larger polymers of length L, one can utilize a simpler but approximate conversion from n to t. If t_n denotes the time since departing the pore after taking n hops, then it follows that $h(L)t_n\approx n$, so that, e.g., $F_{ret}^L[t_n=n/h(L)]\approx F_{ret}^L(n)$. Either the exact or approximate conversion procedure shows clearly how the dependence on polymer diffusivity absent in the discrete-time formulation reappears in continuous-time formulation.

Combining the information in the introduction to Sec. IV regarding growth cycles with these waiting time distributions allows determination of $N_L(t)$. See the Appendix and Sec. V.

C. Non-Markovian kinetics

Traditional Markovian treatments of chemical kinetics assume (often implicitly) exponential waiting-time distributions, or at least finite mean waiting times. The former is required for traditional Markovian kinetics to apply for all times,[23] whereas the latter suffices for long-time Markovian kinetics.[34] However, the key observation for our polymerization model based on either a discrete-time (Sec. IV A) or continuous-time (Sec. IV B) formulation is that the return-time distribution is strongly nonexponential with a slowly decaying long-time tail. In fact, the mean return time diverges for increasing polymer length. Our key claim is that this divergence underlies the failure of a standard Markovian rate equation description of the behavior of the polymer length distribution in the second stage of polymerization. The extrusion-time distribution is also nonexponential, but since extrusion of long polymers is rare, this is not so significant for overall behavior. This claim is rigorously confirmed in the following Sec. V for a simplified version of our polymerization model with maximal catalyst loading.

While we described above the possibility to directly reconstruct the polymer length distributions from waiting-time distributions and information on growth cycles, it is natural to consider development of appropriate evolution equations for the polymer length distribution. Development of an integral equation with non-Markovian memory kernels is possible for the model considered here, although reduction to a simpler non-Markovian generalized master equation (GME) is problematic. See the Appendix.

V. POLYMERIZATION WITH MAXIMAL CATALYST LOADING: KMC SIMULATION AND ANALYTIC RESULTS FOR A SIMPLIFIED MODEL

To distill the essence of the scaling behavior of the polymer length distribution for maximal catalysts loading $L_c=1$ presented in Sec. III, it is instructive to consider a further simplified or tailored version of the model in Sec. IV. The analysis of Sec. III A comparing Figs. 3(b) and 4(a) already

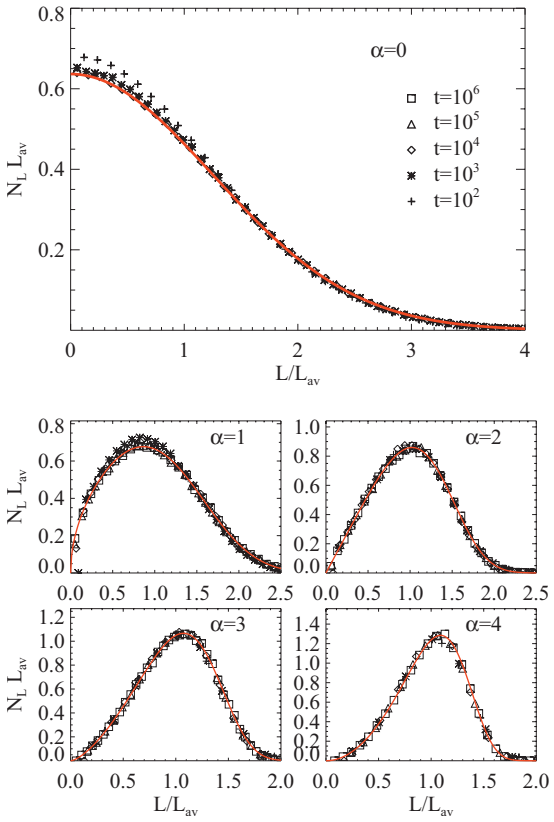

FIG. 6. Evolution of the scaled polymer length distribution the tailored model for catalytic polymerization with maximal catalysts loading ($L_c=1$) and without complete extrusion. The area under the curves corresponds to $N_p=1$ in this analysis. Simulation results for various α shown. Times are shown in the plots. Analytic forms for the scaled distributions are also shown as continuous curves.

demonstrated that complete extrusion (which occurs with low probability for large L) does not significantly influence scaling behavior. Thus, we consider a model where the polymer can wander arbitrarily far from the end of the semi-infinite pore without triggering complete extrusion, i.e., we set $P_{ret}(L)=1$ and $P_{ex}(L)=0$. We retain the form $h(L)=h_m/L^{\alpha}$ for the size dependence of polymer diffusivity. In addition, for simplicity, we specify that the polymer grows by length $\delta L=1$ each time it returns to the pore. Again in this model for a semi-infinite pore, we regard the number of polymers per pore as satisfying $N_p=1$.

A. KMC simulation results

KMC simulation analysis of the above tailored model reveals dynamic scaling of the average polymer length of the form, $L_{av}\sim t^{1/(\alpha+2)}$ entirely consistent with results for the general model described in Sec. III. More detailed analysis reveals that the polymer length distribution, $N_L(t) \propto f(L/L_{av})$ displays perfect scaling for all choices of $\alpha \geq 0$. More specifically, $f(x)=f_{\alpha}(x)$ is independent of t, but its shape depends strongly on α. See Fig. 6. The last feature is of interest since we have noted in Sec. IV A that the polymer length distribution measured after a fixed cumulative number of polymer hops, $N_L(n)$, is independent of α.

B. Exact analysis in the discrete time picture (time in hops)

In this analysis, we replace the general return-time distribution $F^L_{ret}(n)$ described in Sec. IV A by F_n in Eq. (6) corresponding to the classic 1D RW. It is clear that for the above tailored model, $N_L(n)$ is simply determined by the probability that a 1D random walker has returned to the origin exactly $L-L_0$ times after n hops, where L_0 denotes the initial length of the polymer. One has the normalization $\Sigma_L N_L(n)=1$. Likewise, if $L_{av}(n)=\Sigma_L L N_L(n)$ denotes the average polymer length after n hops, then $L_{av}(n)-L_0$ corresponds to the average number of times, M_n, that a 1D random walker returns to the origin after n hops. M_n can be determined exactly from a generating function analysis of the 1D RW problem.[22,30,35] We do not present the details of this type of analysis, but just provide the key results. Let P_n denotes the probability that the 1D RW is at the origin after n hops. Then, one has that[23]

$$P_{2m}=2^{-2m}(2m)!/(m!)^2 \sim \pi^{-1/2}m^{-1/2}, \quad \text{for large m, and} \quad P_{2m+1}=0. \tag{7}$$

A simplistic analysis is based on the claim that the average number of returns after $n=2m$ hops must scale like $M_{2m} \sim m$ $P_{2m}\sim m^{1/2}$.[30] Consistently, a more detailed analysis shows that the number of returns is given exactly by $M_n=\Sigma_{0\leq k\leq n}P_k$.[35] Then, from the latter identity, it follows that

$$\begin{aligned} L_{av}(2m \text{ or } 2m+1)-L_0 &= \sum\nolimits_{0\leq k\leq 2m} P_k = 2^{-2m}(2m+1)!/(m!)^2 - 1 \\ &\sim 2(m/\pi)^{1/2}, \quad \text{for large m}. \end{aligned} \tag{8}$$

A more complete analysis reveals that (cf. Refs. 35 and 36)

$$\begin{aligned} N_L(n) &\sim 2^{1/2}(\pi n)^{-1/2}\exp[-(L-L_0)^2/(2n)] \\ &\sim 2\pi^{-1}(L_{av}-L_0)^{-1}\exp[-\pi^{-1}(L-L_0)^2/(L_{av}-L_0)^2] \\ &\sim 2\pi^{-1}(L_{av})^{-1}\exp[-\pi^{-1}(L/L_{av})^2], \end{aligned} \tag{9}$$

using that $(L_{av}-L_0)^2\sim(L_{av})^2\sim 2\pi^{-1}n$ from Eq. (8). We caution that one should not compare the result (9) with the form (1) to extract f(x) since the meaning of L_{av} is different [sampling for fixed n in Eq. (9) versus fixed t in Eq. (1)].

C. Simple partial analysis in the CTRW picture

First, it is instructive consider the special case where the polymer diffusion coefficient is independent of length, i.e., $h(L)=h_m$ so $\alpha=0$. Then, since the physical time is asymptotically proportional to the number of hops, $h_m t\approx n$, the results from Sec. V B immediately determine the time dependence of key quantities as $t\to\infty$, i.e.,

$$L_{av}(t) - L_0 \sim (2h_m t/\pi)^{1/2} \tag{10a}$$

and

$$N_L(t) \approx 2^{1/2}(\pi h_m t)^{-1/2}\exp[-(L\text{-}L_0)^2/(2h_m t)] \quad \text{for} \quad \alpha = 0. \tag{10b}$$

The result for L_{av} is consistent with simulation results and the simple analysis for $\alpha=0$ in Sec. III A. The result (10a) for $N_L(t)$ implies that $f(x) \approx 2\pi^{-1}\exp(-\pi x^2)$ for $\alpha=0$ which matches exactly the simulation results for the simplified model shown in Fig. 6(a).

Next, we provide a simplified analysis of L_{av}-behavior for the general case where the polymer hop rate decreases with size, $h(L)=h_m L^{-\alpha}$ with $\alpha>0$. From Sec. V B, the mean length of the polymer $L_{av}(t)$ for long times t (where $L_{av} \gg L_0$) scales like the square root of the total number of polymer hops, n, which is roughly given by $n \approx \int_{0<t'<t} dt'\ h(L(t'))$. Thus, one concludes that

$$[L_{av}(t)]^2 \sim \int_{0<t'<t} dt' [L_{av}(t')]^{-\alpha}. \tag{11}$$

Assuming that $L_{av} \sim t^{\beta}$ for large t, substitution into Eq. (11) implies that $2\beta=-\alpha\beta+1$. This in turn implies that $\beta=1/(\alpha+2)$ consistent with the rate equation analysis of Sec. III. It is not possible to determine the polymer length distribution $N_L(t)$ from such a simplified analysis. Instead, the more complicated treatment in the following Sec. V D is required.

Finally, we should note that the above estimate for the total number of hops until time t is somewhat simplistic given the unusual nature of the distribution of return times which derives from the long-tail in F_n.[30] A more precise analysis is provided in Sec. V D. However, for purposes of analysis of the asymptotic behavior of L_{av}, we note that an even simpler estimate of the number of hops up to time t as $n \approx h(L(t)) \cdot t$ suffices to produce the correct exponent $\beta=1/(\alpha+2)$.

D. General analysis in the CTRW picture: Formalism

Within this general CTRW analysis, we specify a return-time distribution of the form

$$F_{ret}^{L}(t) = h(L) F_{ret}(h(L)t), \tag{12a}$$

where

$$\int_{0<u<\infty} du\ F_{ret}(u) = 1 \quad \text{and} \quad F_{ret}(u) \sim u^{-3/2}/(2\pi)^{1/2} \quad \text{for large } u. \tag{12b}$$

A precise and general continuous-time analysis of this tailored model follows from determination of a general waiting-time density, $\psi_n(t)$. Here, $\psi_n(t)dt$ gives the probability that the polymer of initial length L_0 returns to the pore for the nth time between times t and t+dt, and thus grows to length $L=n+L_0$. We also set $\psi_0(t)=\delta(t)$, the Dirac delta function. It is immediately clear that $\psi_n(t)$ is determined from the return-time distributions for polymers of various lengths, which have the form described above in Eq. (12). Specifically, it follows that

$$\psi_n(t) = \int_{0<t'<t} dt' \psi_{n-1}(t') F_{ret}^{L-1}(t-t'), \quad \text{where} \quad n = L - L_0 \geq 1. \tag{13}$$

Also let $\Psi_L(t)=1-\int_{0<t'<t} dt' F_{ret}^{L}(t')$ denote the probability that a polymer of length L does not return within a time t after departing the pore. Then, the probability to find a polymer of length L at time t is given by

$$N_L(t) = \int_{0<t'<t} dt' \psi_{n=L-L_0}(t') \Psi_L(t-t'). \tag{14}$$

This expression reflects the scenario where the polymer returns to the pore for the nth time with $n=L-L_0$ to grow to length L at time t′, and also that it does not return again in the time interval from t' to t. Analysis of Eqs. (14) and (13) is naturally achieved via Laplace transformation. If we define $\tilde{N}_L(s)=\int_{0<t<\infty} dt\ e^{-st} N_L(t)$, then such an analysis reveals that

$$\begin{aligned}\tilde{N}_L(s) &= \tilde{\psi}_{n=L-L0}(s)\tilde{\Psi}_L(s) \\ &= \tilde{F}_{ret}^{L-1}(s)\tilde{F}_{ret}^{L-2}(s)\cdots\tilde{F}_{ret}^{L0}(s)[1-\tilde{F}_{ret}^{L}(s)]/s \\ &= s^{-1}[1-\tilde{F}_{ret}(s/h(L))]\Pi_{L0\leq K\leq L-1}\tilde{F}_{ret}(s/h(K)),\end{aligned} \tag{15}$$

where $\tilde{F}_{ret}(s)=\int_{0<u<\infty} dt\ e^{-su} F_{ret}(u)$ and the second equality uses Eq. (12a). Inversion of this Laplace transform would yield the desired distribution $N_L(t)$.

E. General analysis for the CTRW picture: Results

In analyzing Eq. (15), it is instructive to first reconsider the simplest case where the polymer diffusion coefficient is independent of length, i.e., $h(L)=h_m$ so $\alpha=0$. Here, we already have results (10b) from the simplified analysis in Sec. V C. In this case, Eq. (15) becomes[37]

$$\tilde{N}_L(s) = s^{-1}[1-\tilde{F}_{ret}(s/h_m)][\tilde{F}_{ret}(s/h_m)]^{L-L_0}, \quad \text{for} \quad L \geq L_0 \quad \text{and} \quad \alpha = 0. \tag{16}$$

Defining $\delta L_{av}(t)=L_{av}(t)-L_0$ and $\delta\tilde{L}_{av}(s)=\int_{0<t<\infty} dt \times e^{-st}\delta L_{av}(t)$, it follows that[37]

$$\delta\tilde{L}_{av}(s) = s^{-1}\tilde{F}_{ret}(s/h_m)[1-\tilde{F}_{ret}(s/h_m)]^{-1}, \quad \text{for} \quad \alpha = 0. \tag{17}$$

Since $\int_{0<u<\infty} du\ F_{ret}(u)=1$ and $F_{ret}(u) \sim u^{-3/2}/(2\pi)^{1/2}$ for large u, it follows that[38]

$$1-\tilde{F}_{ret}(s/h_m) \sim 2^{1/2}(s/h_m)^{1/2} \quad \text{as} \quad s \to 0. \tag{18}$$

From this result, one immediately obtains

$$\delta\tilde{L}_{av}(s) \sim 2^{1/2}(h_m)^{1/2}s^{-3/2}, \quad \text{so} \quad L_{av}(t) \sim \delta L_{av}(t) \sim 2^{1/2}\pi^{-1/2}(h_m t)^{1/2}, \quad \text{for} \quad \alpha = 0, \tag{19}$$

recovering the result from Sec. V C which was based on a cruder approximate analysis.

Determination of the polymer length distribution is more complicated. It is convenient to use the relation $(1-a)^M \approx \exp(-aM)$ for $M \gg 1$ and $a \ll 1$ with $aM=O(1)$ to rewrite Eq. (16) as

$$\tilde{N}_L(s) \sim 2^{1/2}(h_m)^{-1/2}s^{-1/2}\exp[-2^{1/2}(L-L_0) \times (s/h_m)^{1/2}] \quad \text{for} \quad \alpha = 0. \tag{20}$$

From Eq. (19), it follows that[39]

$$N_L(t) \sim (2/\pi)^{1/2}(h_m t)^{-1/2}\exp[-(L-L_0)^2/(2h_m t)] \quad \text{for} \quad \alpha = 0, \tag{21}$$

consistent with Eq. (10b) in Sec. V C.

Finally, we consider the general case of polymer diffusion coefficient decreasing with length, i.e., $\alpha > 0$. Naturally, inversion of the Laplace transform (15) is more complicated than in the simple case where $\alpha=0$. However, one can still perform an approximate analysis again using $(1-a)^M \approx \exp(-aM)$, and for simplicity regarding $L_{av} \gg L_0$, to obtain

$$\begin{aligned}\tilde{N}_L(s) &\approx 2^{1/2}h(L)^{-1/2}s^{-1/2}\exp[-2^{1/2}s^{1/2}\{h(L_0)^{-1/2} + h(L_0+1)^{-1/2} + \cdots + h(L-1)^{-1/2}\}] \\ &\approx 2^{1/2}h(L)^{-1/2}s^{-1/2}\exp[-2^{3/2}(\alpha+2)^{-1}(s/h_m)^{1/2}L^{1+\alpha/2}].\end{aligned} \tag{22}$$

The result (22) implies that[39]

$$\begin{aligned}N_L(t) &\approx \pi^{-1/2}2^{1/2}h(L)^{-1/2}t^{-1/2}\exp[-2(\alpha+2)^{-2}L^{\alpha+2}/(h_m t)] \\ &\approx [a(\alpha)/L_{av}](L/L_{av})^{\alpha/2}\exp[-b(\alpha)(L/L_{av})^{\alpha+2}],\end{aligned} \tag{23}$$

where $L_{av} \sim (h_m t)^{1/(\alpha+2)}$, and $b(\alpha)$ and $a(\alpha)$ follow immediately from normalization and mean value constraints. This result is perfectly consistent with simulated distributions in Fig. 6, and succeeds in providing a sophisticated derivation of the dynamic scaling of L_{av}. Interestingly, it reveals a generalized gamma distribution form for the scaling function $f(x)$ with faster-than-Gaussian decay for $\alpha > 0$ for the regime of large polymer lengths.

VI. SUMMARY

We have discovered an unusual non-Markovian scaling behavior of the polymer length distribution for catalytic polymerization in a mesoporous system in the regime of growth where polymers are partially extruded from the pores. Results are shown primarily for the case $\alpha=3$, but our simulations reveal essentially the same behavior for any $\alpha \geq 1$. We demonstrate that this behavior is a direct consequence of the long-time tail in the return-time distribution for the end of the polymer to return to the pore. This connection is made utilizing the methodology of CTRW theory.

We also noted that standard Markovian rate equations describe at least qualitatively behavior in the growth regime where the polymer remains within the pore. However, sharpening of the distribution predicted by such equations is greater than that observed in simulations. This quantitative discrepancy is also readily understood. The mean return-time for the end of the polymer to return to the same or a neighboring catalytic site within the pore is finite. However, the return-time distribution is not exponential, so Markovian behavior should not apply for all times. In fact, for lower catalyst loadings where L_c is larger, the return-time distribution has a long tail for a broad range of times. This long-tail is cut off only around the quite long mean return time. Thus, initial growth behavior is expected to exhibit non-Markovian features.

Finally, it is appropriate to note that there are numerous generalizations and extensions of our catalytic polymerization models for which growth behavior might be analyzed. One example of particular relevance here is to consider the cases where there is a finite driving force for polymer extrusion. Then, at least for partially extruded polymers, there is a bias in their diffusion favoring the direction out of the pore. Analysis of the return-time distribution for the end of the polymer to the pore prompts consideration of the behavior of simple biased 1D RWs. The bias means that there is a finite probability that the RW will not return to the origin, i.e., the RW is not recurrent.[23] However, the conditional mean return time, i.e., the return time determined for those trajectories which do return to the origin, is now finite, in contrast with the classic unbiased case.[23] (The property of having a finite mean return time is referred to as "strong transience," a feature which holds for biased but not unbiased walks.) As a consequence of this strong transience, one expects that a Markovian rate equation treatment for the polymer length distribution (accounting for the now significant probability of complete extrusion) will at least qualitatively predict model behavior.

ACKNOWLEDGMENTS

This work was supported by the Division of Chemical Sciences (Basic Energy Sciences), USDOE. Theory development and modeling studies were supported through the Ames Laboratory PCTC and Chemical Physics projects, respectively. Ames Laboratory is operated for the USDOE by Iowa State University under Contract No. DE-AC02-07CH11358.

APPENDIX: MODEL ANALYSIS FOR MAXIMAL CATALYST LOADING

We provide a brief but more comprehensive overview of different formulations for the model in Sec. IV with maximal catalyst loading $L_c=1$:

(i) Discrete "growth cycle" picture. First recall the introduction to Sec. IV where we described tracking behavior in terms of growth cycles, i.e., the cumulative number of the returns of the polymer to the pore plus the number of complete extrusions. This provides a discrete growth cycle (C) picture of the polymer growth process as a stochastic walk in the state space of polymer length L (cf. Refs. 23 and 29). In each cycle $C=1,2,3,\cdots$, i.e., after each return to the pore (or complete extrusion), one allows transitions in polymer length

$$L \to L+m \text{ with probability } p_m P_{ret}(L) \quad \text{for } m \geq 1, \quad \text{and} \quad L \to 2 \quad \text{with probability } P_{ex}(L). \tag{A1}$$

It is then a simple matter to recursively determine the polymer length distribution, $N_L(C)$, at growth cycle C using the transition rules (A1) and given an initial length L_0 (cf. Refs. 23 and 29).

(ii) Discrete-time picture. As in Sec. IV A, "time" can be measured in terms of the cumulative number of hops "n" taken by the partially extruded polymers. The number of hops, n, corresponds to a much finer time scale than the growth cycle number, C, since typically many hops are made each cycle. Combining the transition probabilities (A1) with the discrete-time return and extrusion time distributions introduced in Sec. IV A, in principle, allows determination of $N_L(n)$. This is analogous to the continuous-time treatment in Sec. V for the simplified model.

(iii) Continuous-time picture. As seen in Sec. IV B, one can directly introduce continuous-time return and extrusion time distributions. Combining the transition probabilities (A1) with these continuous-time time distributions in principle allows determination of $N_L(t)$, analogous to the treatment in Sec. V. Again, this CTRW formulation is preferred for comparison with results from KMC simulation and experiment.

As indicated in Sec. IV C, it is natural to attempt to develop evolution equations for $N_L(t)$ within the CTRW formulation. Slightly refining the standard CTRW development, we claim that the population $N_{L,L_0}(t)$ of polymers of length L at time t given an initial length L_0 satisfies

$$N_{L,L_0}(t) = \delta_{L,L_0}\Psi_{L_0}(t) + \sum_{m\geq 1} p_m \int_{0<t'<t} dt' F_{ret}^{L_0}(t') \times N_{L,L_0+m}(t-t') + \int_{0<t'<t} dt' F_{ex}^{L_0}(t') N_{L,2}(t-t'), \tag{A2}$$

where $\Psi_{L_0}(t) = 1 - \int_{0<t'<t} dt' F_{ret}^{L_0}(t') - \int_{0<t'<t} dt' F_{ex}^{L_0}(t')$ is the probability that no transition occurs from $L=L_0$ over a time period t, and where for convenience N_{L,L_0} is normalized to unity (cf. Ref. 23). This formulation explicitly enumerates all possibilities for the first transition from the polymer length L_0 to length $L'=L_0+m$ or to length $L'=2$ at time t'. Subsequent (generally) multiple transitions leading from length L' to L by time t are described by $N_{L,L'}(t-t')$-factors. Somewhat unconventionally, for $L_0=2$, the last term in Eq. (A2) accounts explicitly in for "transitions" from $L_0=2$ to $L=2$ by complete extrusion and creation of a new two-unit polymer. We correspondingly reduced $\Psi_{L_0}(t)$. One cannot ignore this transition as complete extrusion "resets the clock" on the waiting-time distribution for return to the pore.

The long time-tail in the memory kernel $F_{ret}^{L_0}(t')$ in Eq. (A2) for large L induces the breakdown of Markovian treatments. The most detailed analysis of evolution equations of the form (A2) is in the special case with waiting-time distributions independent of the initial state. Then, a Laplace transform analysis reveals that the solution evolves according to a non-Markovian generalized master equation (GME).[22] The GME memory kernel is directly related to but distinct from the waiting-time distribution. Furthermore, infinite waiting times induce "anomalous" regimes of negative values for this memory kernel.

[1] K. Tajima and T. Aida, *Nanostructured Catalysts* (Plenum, New York, 2003).
[2] V. S.-Y. Lin, D. R. Radu, M.-K. Han, W. Deng, S. Kuroki, B. H. Shanks, and M. Pruski, J. Am. Chem. Soc. **124**, 9040 (2002).
[3] S. Huh, J. W. Wiench, J.-C. Yoo, M. Pruski, and V.-S.-Y. Lin, Chem. Mater. **15**, 4247 (2003).
[4] J. Kärger and D. Freunde, Chem. Eng. Technol. **25**, 769 (2002).
[5] D. S. Sholl and K. Fichthorn, Phys. Rev. Lett. **79**, 3569 (1997).
[6] D. Dubbeldam, S. Calero, T. L. M. Maesen, and B. Smit, Phys. Rev. Lett. **90**, 245901 (2003).
[7] D. J. Liu, H.-T. Chen, V. S.-Y. Lin, and J. W. Evans, Phys. Rev. E **80**, 011801 (2009).
[8] P. G. de Gennes, *Scaling Concepts in Polymer Physics* (Cornell UP, Ithaca, 1979).
[9] A. Baumgartner and M. Muthukumar, Adv. Chem. Phys. **94**, 625 (1996).
[10] H. Mori, Prog. Theor. Phys **33**, 423 (1965).
[11] R. Zwanzig, *Nonequilibrium Statistical Mechanics* (Oxford, New York, 2001).
[12] R. Kubo, Rep. Prog. Phys. **29**, 255 (1966).
[13] R. Balescu, *Equilibrium and Nonequilibrium Statistical Mechanics* (Wiley, New York, 1975).
[14] S. V. Nedea, A. P. J. Jansen, J. J. Lukkien, and P. A. J. Hilbers, Phys. Rev. E **65**, 066701 (2002); **66**, 066705 (2002).
[15] This time unit corresponds to the physical time for the root-mean-square displacement of a diffusing monomer to equal the length of the monomer.
[16] K. Kang and S. Redner, Phys. Rev. Lett. **52**, 955 (1984).
[17] K. Kang and S. Redner, Phys. Rev. A **30**, 2833 (1984).
[18] R. M. Ziff, E. Gulari, and Y. Barshad, Phys. Rev. Lett. **56**, 2553 (1986).
[19] K. A. Fichthorn and W. H. Weinberg, J. Chem. Phys. **95**, 1090 (1991).
[20] J. W. Evans, D.-J. Liu, and M. Tammaro, Chaos **12**, 131 (2002).
[21] *On Growth and Form*, edited by H. E. Stanley and N. Ostrowsky (Martinus Nijhoff, Dordrecht, 1986).
[22] E. W. Montroll and G. H. Weiss, J. Math. Phys. **6**, 167 (1965).
[23] B. D. Hughes, *Random Walks and Random Environments* (Oxford Science, Oxford, 1995), Vol. 1.
[24] Due to the recurrence of 1D random walks (Ref. 23), the end of the polymer is far more likely to return to the same catalyst site after $n_h \sim L_c$ hops, rather than to reach an adjacent catalyst site after $n_h \sim (L_c)^2$ hops. The mean number of hops to reach any catalyst site satisfies $\langle n_h \rangle \approx L_c$.
[25] The residence time of the end of the long polymer of length L at the catalytic site, $\tau_{poly}=1/h(L)$ far exceeds the characteristic time, $\tau_m = 1/h_m = 1$, for monomer hopping. Thus, even for small monomer densities, there is usually sufficient time for monomers to reach the catalytic site and react before the polymer hops. As a result, typically one has that $P_{rx} \approx 1$.
[26] D.-J. Liu and J. W. Evans, Phys. Rev. B **66**, 165407 (2002) (See the Appendix.).
[27] The loss term in d/dtL_{av} due to extrusion has the form $-P_{ex}L_{av}h(L_{av})/\langle n_h \rangle|_{L=Lav}$ noting that the length of the polymer is reduced from $L \sim L_{av}$ to $L \sim O(1)$ upon extrusion.
[28] Using the notation in the Appendix, these Markovian equations have the form $d/dt\ N_L = \Sigma_{m>0} p_m [P_{ret}(L-m)R_{ret}(L-m)N_{L-m} - P_{et}(L)R_{ret}(L)N_L] - P_{ex}(L)R_{ex}(L)N_L$, for $L>2$, and $d/dtN_2 = \Sigma_{L'>2} P_{ex}(L')R_{ex}(L')N_{L'} - P_{ret}(2)R_{ret}(2)N_2$. The equations also involve rates for return, $R_{ret}(L)$, and extrusion, $R_{ex}(L)$, of a polymer of length L.
[29] G. H. Weiss and R. J. Rubin, Adv. Chem. Phys. **52**, 363 (1983).
[30] S. Redner, *A Guide to First-Passage Processes* (Cambridge UP, Cambridge, 2001).
[31] From Ref. 30, the behavior of F_n also follows from that of the "survival

probability" of not returning after n steps, $S_n \sim n^{-1/2}$ and the relation $S_n = 1 - \Sigma_{m \le n} F_n$.
[32] The generating function for nF_n satisfies $zF'(z) \sim 2^{-1/2}(1-z)^{-1/2}$ as $z \to 1$. Application of the discrete Tauberian Theorem (Ref. 23) implies that $n\ F_n \sim 2^{-1/2} n^{-1/2}/\Gamma(1/2)$, for even $n \to \infty$.
[33] The conditional mean return time sampling only those walks which return in the first n steps diverges like $(2n/\pi)^{1/2}$ (Ref. 23) consistent with stated large n-behavior of F_n.
[34] D. Bedeaux, K. Lakatos-Lindenberg, and K. E. Shuler, J. Math. Phys. **12**, 2116 (1971).
[35] M. Ferraro and L. Zaninetti, Phys. Rev. E **64**, 056107 (2001). This analysis appears to start from an invalid equation, although correctly recovering Eq. (8).
[36] The analysis is also presented in Ref. 30, but the result is missing a factor of 2.
[37] This result follows from a conventional CTRW analysis (Ref. 23).
[38] This result follows using the strong Tauberian theorem (Ref. 23) to relate $t\ F_{ret}(t) \sim t^{-1/2}/(2\pi)^{1/2}$ to its Laplace transform $-d/ds\tilde{F}_{ret}(s)$.
[39] This relationship between $\tilde{N}_L(s)$ and $N_L(t)$ follows from consideration of the Laplace transform of the Gaussian solution to the standard continuum diffusion equation.